



Experiment title:
Phase transition from the photonic glass to the photonic crystal

Experiment number:
HC-1952

Beamline:
BM26B

Date of experiment:
from: 11/06/2015 to: 15/06/2015

Date of report:
21.02.2017

Shifts:
12

Local contact(s): Daniel Hermida Merino

Received at ESRF:

Names and affiliations of applicants (* indicates experimentalists): **A.Chumakova (PNPI), A. Chumakov (PNPI), A. Mistonov*(SPbSU), I. Shishkin* (SPbSU).**

Report:

To produce the photonic materials we have used a new method, which prototype is known in ceramic technology as a slip casting. It has provided the systems consisting of monodisperse spherical particles with different extent of positional order, ranging from the photonic glasses through structures with short-range order to photonic crystals. We have studied the structure of sample series prepared in the different technological conditions (deposition rate, orientation of deposition plane) and estimated the parameters on the structural transformation.

As an original solution colloidal solution of polystyrene spheres with diameter of 200 ± 5 nm in aqueous medium with 6.5% volume fraction was selected. Varying the rate of absorption of the colloidal solution by the gypsum cell the several series of photonic materials were prepared. Each of the series consisted of three samples types which depended on the direction of film growth plane relative to the gravitational force: codirectional, against and perpendicular to the direction of growth. The film thickness was about 2 mm and depended on the series.

The typical microphotographies was obtained with chip of photonic structure with short-range order and photonic crystal with long-range order (Fig.1) by Scanning Electron Microscopy (SEM). In doing so, we have observed disorder-order transition of photonic 3D materials.

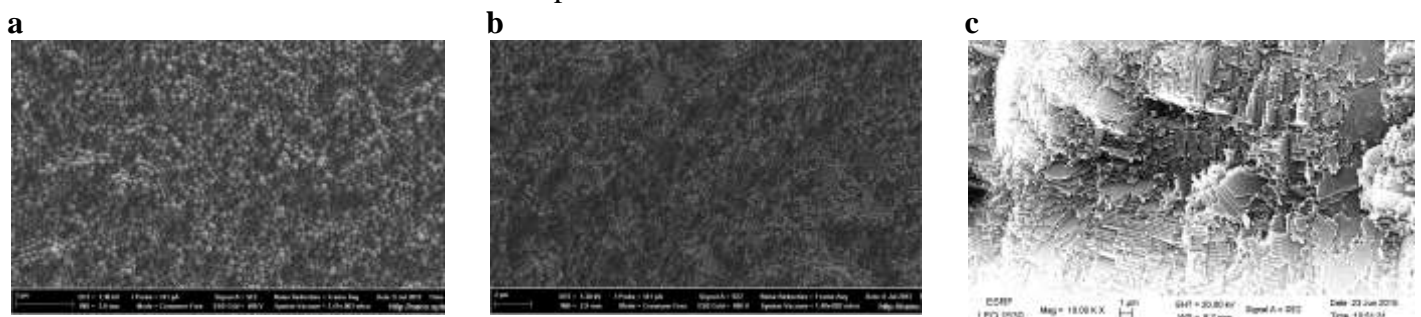


Fig.1. Typical Scanning Electron Microscopy images of (a) photonic glass and (b) polycrystalline structure with photonic short-range order and long-range order obtained by slip casting method

During the experiment, the monochromatic X-ray beam incidented on the sample and the scattered waves were recorded in a two-dimensional diffraction pattern, which contains the rings from disorder structure obtained at large deposition rate, Fig. 2. Stepwise scanning along the film thickness obtained by a series of diffraction patterns at different positions were performed. X-ray beam was incident close to the sharp top side of a triangular prism sample formed by the initial deposition point "S" (start of the synthesis with maximal speed) to the opposite side of "F" (finish of the synthesis with minimal speed). As the displacement of X-ray beam to the finish of synthesis, the diffraction peaks began to appear on the rings of different orders, this peaks were broadened in the azimuthal direction and showed sixfold symmetry.

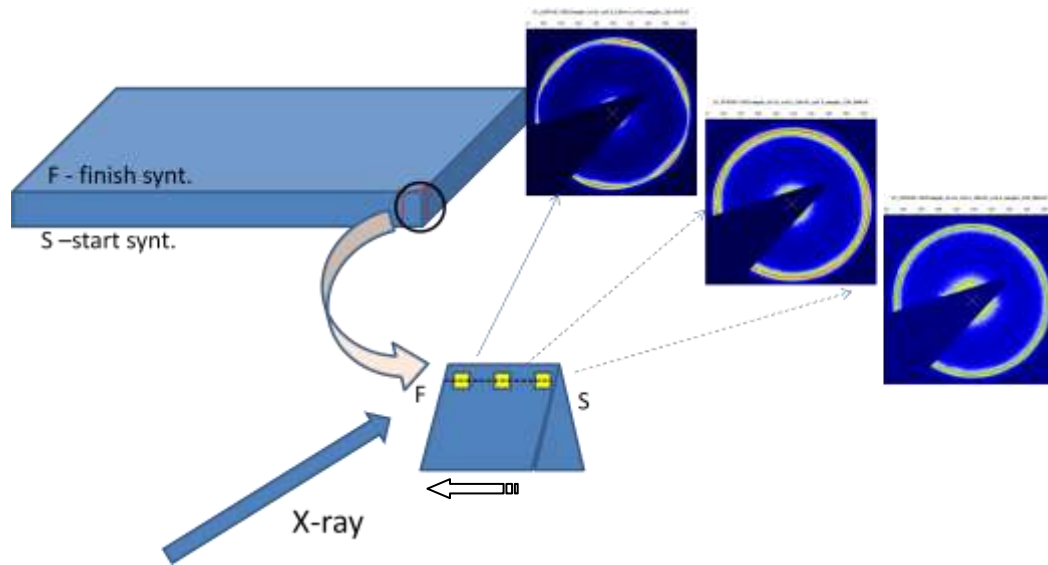


Fig 2 – Geometry of SAXS experiment for the study of samples splinters of the artificial opal-like structure.

The intensity distribution in the diffraction patterns were analyzed in the azimuthal and radial directions. The data presented in Fig.3 show a typical distribution of the first order peak intensity in the azimuthal direction from the polycrystalline structure, which indicates the directional growth of crystallites with increasing thickness of the sample. The full width at half maximum (FWHM) W_{az} , averaged over several peaks in a single ring, shown in Fig. 3 (b). Reducing the azimuthal width of the peak with the growth of the film indicates the predominance of the directional growth of crystallites in the samples.

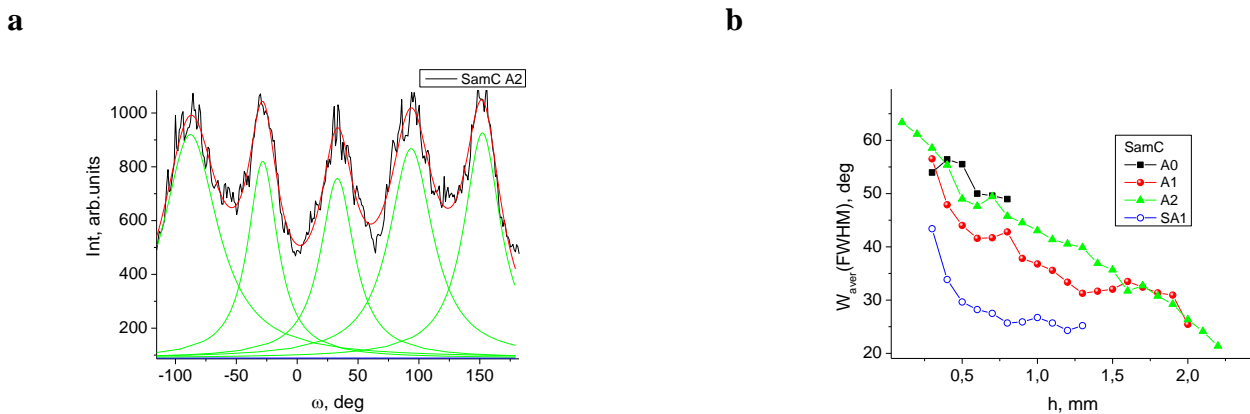


Fig.3. The analysis of experimental data using the sum of Lorentz functions for the first order peaks in azimuthal direction of SamC A2 series at 15 scanning step along the thickness of the sample (a); The averaged widths at half maximum for the azimuthal orientation of the first order peaks for a series of samples A0, A1, A2 and SA1.

An analysis of the radial intensity distribution in the diffraction patterns allows to determine the period of the structure, crystallite size, the presence of different types of defects and structural features of the samples. The typical graph of the radial distribution of the first order peak intensity is shown in Fig. 4 (A). The main peak centered at $Q_1 = 0.03376 \text{ nm}^{-1}$ and the width $dQ = 0,00268 \text{ nm}^{-1}$ is a satellite peak in the small-angle region centered $q_{1s} = 0,03521 \text{ nm}^{-1}$. The ratio of provisions of the main and satellite peaks Q_1/Q_{1s} to determine the difference in the distance between the particles to a disordered (amorphous) and polycrystalline phases in the irradiated region of the sample. Here $Q_1/Q_{1s} = 0,95$ and shows that the average distance between the closest neighboring areas in the amorphous phase is at 5% more than in polycrystalline one. The broadening of the small-angle region is absent at the second order rings. It indicates that the rapid decay of the contribution from the disordered component of the irradiated sample volume of the structure, depending on the volume occupied by the rigid spheres.

The ratio of the integral intensities of the main peak to the satellite is shown on Fig 4(b). These curves demonstrate a decrease in the contribution of the amorphous component to a polycrystalline phase with increasing thickness of the sample h and a decrease of deposition rate V for a series of samples A1, A2 and SA1. The broadening of radial distribution intensity of the first order peaks for A0 series of samples obtained at $V > 10^{-3} \text{ ml/s/cm}^2$ does not allow clearly divide the above contributions.

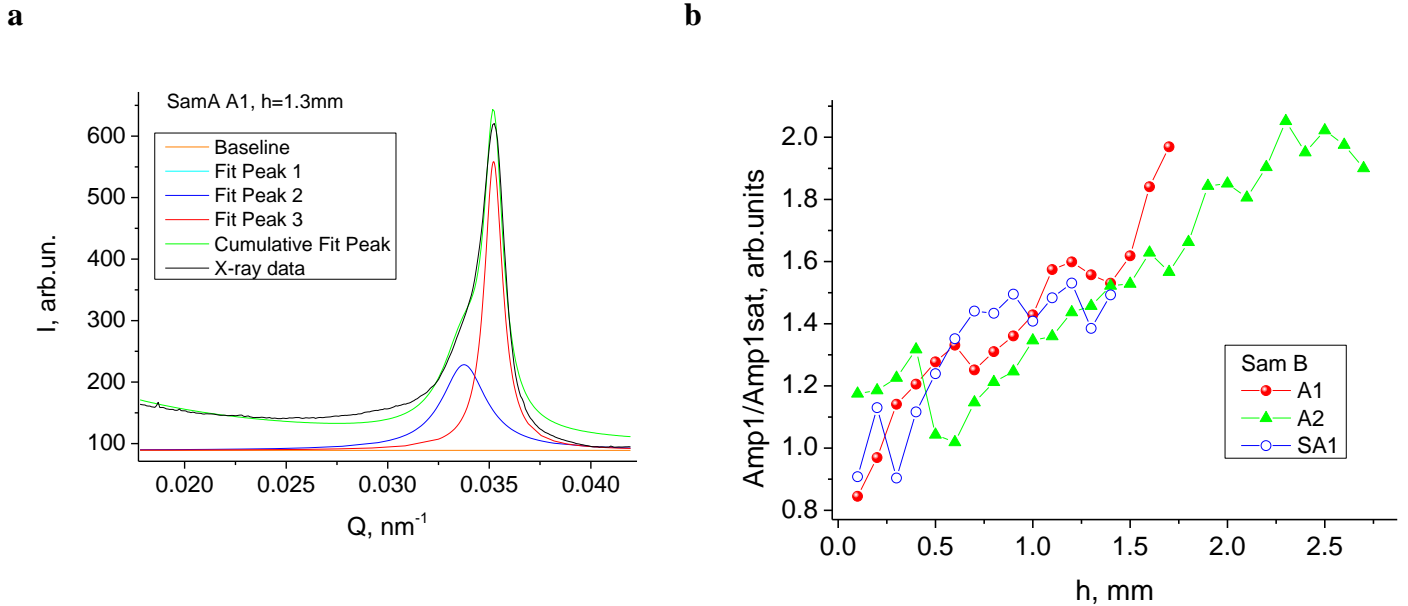


Fig.4. - The radial distribution of the first order peak intensity resulting from the illuminated region A1 SamA sample series at the distance of 1.3 mm from the "S" edge (a). The ratio of the integrated intensities of the main peak of the first order to the satellite (b).

Fig. 5 shows examples of analysis results of experimental data (diffraction patterns), it see that with the increasing thickness of sample the crystallite size increase, that testify the directional growth of crystallites. During the analysis of radial intensity distribution in the diffraction patterns to determined the structure period $a_0 = 183 \pm 4 \text{ nm}$, and crystallite size of ordered part structure, which are changing from 10 to 30 structure period (1,5 -5,5 μm).

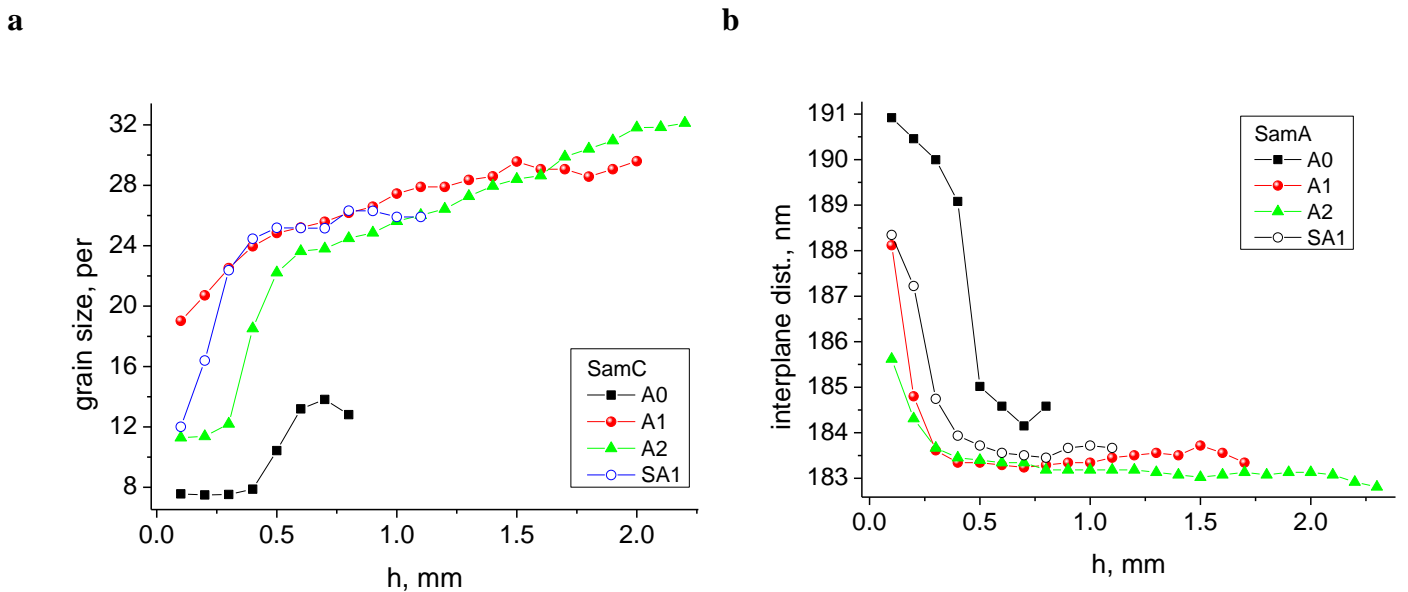


Fig.4. - The dependence of the change in volume-averaged crystallite size in different thicknesses of samples SamB and SamC examined four series of samples, expressed in in the period of the structure (a.) The interplanar distance calculated from the position of the first order peaks for samples SamA of the series A0, A1, A2 and SA1, depending on the location of the sample thickness h (b).

It has been found that the strong disorder structure was mainly produced at absorption rate of solvent $>10^{-3} \text{ ml/sec/cm}^2$, then as colloidal spheres begin to pack to polycrystall structure at the absorption rate $<10^{-4} \text{ ml/sec/cm}^2$. With increase of the thickness of the sample the phase of order revolve with each other (photonic glass \rightarrow polycrystalline structure with short-range order \rightarrow polycrystalline structure with long-range order). The crystallite size depends on the absorption rate and changes from 1,5 μm to 5,5 μm (depending on series samples). The ratio between the amorphous and the order parts of samples can be discribde in terms of the Percus-Yevick model and is 5%.

It should also be noted that rapid ordering of investigating opal-like structures occurs sufficiently fast about the first 0.5 mm of the sample points from the initial synthesis moment then the interplanar spacing varies slightly. Effect of gravitational force on the ordering of the particles were not found with respect to the orientation of the deposition plane.